

Effect of Ambient Turbulence on the Elliptical Instability of a Vortex Pair

Jiratrakul Tunkeaw^{1,*}, Arpiruk Hokpunna¹ and Watchapon Rojanaratanangkule¹

¹Department of Mechanical Engineering, Faculty of Engineering, Chiang Mai University,
239 Huay Kaew Rd., Muang District, Chiang Mai, Thailand, 50200

*Corresponding Author: jiratrakul_earn@hotmail.com, 087-658-7164

Abstract

The effect of ambient turbulence on the elliptical instability and the breakdown process of a counter-rotating vortex pair studied via the use of direct numerical simulation (DNS). The ambient turbulence is modelled as homogeneous isotropic turbulence (HIT). The turbulence intensity is characterised by the turbulence dissipation rate. It is found that the ambient turbulence suppresses the occurrence of the elliptical instability. It alters the most amplified wavenumber from mode $\kappa = 6$ (without ambient turbulence) to $\kappa = 2$. Additionally, the linear regime of the three-dimensional instability is bypassed.

Keywords: Counter-rotating vortex pair, Elliptical instability, Turbulence ambient, Direct numerical simulation

1. Introduction

Once an airplane manoeuvres, it sheds a pair of wake vortices rotating in the opposite direction, which can be found far away behind an airplane 5 – 10 times of wingspan distance [1]. The occurrence of these wake vortices is one of the main problems for the air transportation and airport because it possesses a strong circulation and is long-lived. For example, it may cause a hazard to the following aircraft (especially with a small airplane), resulting in the flight delay [2]. It is thus important to investigate the evolution of the counter-rotating vortex pair to explore its behaviour and predict how long it can live, especially in realistic backgrounds (e.g. stratification, turbulence).

One of the most important dynamics of the vortex pair is that many kinds of three-dimensional instabilities develop during the change from laminar to turbulence. Generally, the vortex pair undergoes laminar-to-turbulence transition via two types of mechanisms, namely the short-wavelength (elliptical) and the long-wavelength (Crow) instability. Both of instabilities can be classified by the vortex aspect ratio (a_o/b_o , where a_o being the vortex core radius and b_o being the separation distance between vortex pair), and it is found that the elliptical instability happens when $a_o/b_o > 0.1$ [3]. When the elliptical instability occurs, it influences the mutual induce strain and vortex stretching of the vortex pair during the linear phase. The vortex pair then undergoes the

nonlinear phase, in which the secondary vortex arises, and finally breaks down to turbulence resulting in a decrease of the vortex circulation [4].

Previous studies in both short-wavelength and long-wavelength instabilities in a stratified fluid found that the elliptical instability develops qualitatively in the same manner as in an unstratified fluid when the stratification is below the moderate level ($\infty \geq Fr \geq 2$, where Fr being the Froude number). For the strong stratification ($Fr < 2$), the buoyancy effect enhances the effect of mutual induce strain and secondary vortex. This increases the rate of the vortex decay [5]. On the other hand, the buoyancy force affects the Crow's instability only when the level of stratification is weak to moderate. This decreases the vortex circulation and reduces the required time for the appearance of the bursting process, which leads to the occurrence of a vortex ring. In the strong stratification, the vortex pair is destroyed before a vortex ring appears [6]. When the Crow's instability develops in the background turbulence, it is found that the bursting process happens faster than that in a stratified fluid. Additionally, the decay rate of the vortex pair increases. This suggests that the effect of the ambient turbulence has more influence than the buoyancy force [7].

Thus, this research investigates the effect of ambient turbulence, modelled as homogeneous isotropic turbulence (HIT), on the development of the elliptical instability via the use of direct numerical simulation (DNS). The effect of the ambient turbulence on the most amplified mode

and the growth rate of the energy spectrum is explored.

2. Numerical Approach

The governing equations of the vortex pair in an incompressible fluid can be written as

$$\frac{\partial u_i}{\partial x_i} = 0, \quad (1)$$

$$\frac{\partial u_i}{\partial t} + u_j \frac{\partial u_i}{\partial x_j} = -\frac{1}{\rho} \frac{\partial p}{\partial x_i} + \nu \frac{\partial}{\partial x_j} \left(\frac{\partial u_i}{\partial x_j} + \frac{\partial u_j}{\partial x_i} \right), \quad (2)$$

Where $x_i = (x, y, z)$ is the Cartesian velocity, $u_i = (u, v, w)$ is the velocity in each direction, t is time, ρ is the fluid density, p is the pressure and ν is the kinematic viscosity. The governing equations are discretised in space by the second-order central differencing scheme on a staggered grid, while the second-order Adams–Bashforth is employed to march the equation in time.

2.1 Initial Condition

Vortex Pair

The simulation of a vortex pair with and without ambient turbulence is performed in a domain of size $2\pi \times 2\pi \times 6\pi$ with the resolution of $128 \times 128 \times 384$. This domain is long enough to study only the effect of elliptic instability while short enough to eliminate the effect of the Crow’s instability [5].

The initial condition of vortex pair is the Lamb–Oseen vortices since it fits well the previous experiment of Leweka et al. [8]. The vorticity distribution in the streamwise direction (ω_y) of the Lamb–Oseen vortices is

$$\omega_y(x, y, z) = \Omega_o \exp \left[-\frac{(x-x_1)^2 + (z-z_1)^2}{a_o^2} \right] - \Omega_o \exp \left[-\frac{(x-x_2)^2 + (z-z_2)^2}{a_o^2} \right] \quad (3)$$

Where $\Omega_o = \Gamma_o / \pi a_o^2$ is the maximum vorticity, Γ_o is the initial circulation and a_o is the initial vortex core radius. The quantities x_i and z_i are the initial centre of each vortex and we set $z_1 = z_2 = 0$. The initial separation distance is $b_o = |x_1 - x_2| = 1$,

while the initial descent velocity of vortex pair is defined as $W_o = \Gamma_o / 2\pi b_o = 1$. The vortex dipole aspect ratio at which the elliptic instability to occur is $a_o / b_o = 0.177$. The Reynolds number is defined from the initial circulation as $Re_\Gamma = \Gamma_o / \nu = 2400$. The random perturbation is added to the initial velocity field with the amplitude of $0.001W_o$. Note that all the initial values given above are the same as those of Nomura et. al [5] who investigated the effect of the stratification on the development of the elliptical instability of the vortex pair. The initial structure of the vortex pair and the coordinate system are displayed in Figure 1.

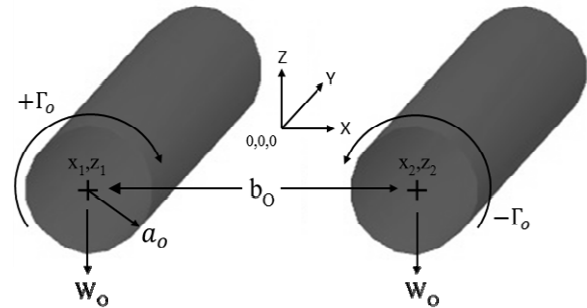


Figure 1. The initial structure and coordinate system of the vortex pair.

Ambient Turbulence

The homogeneous isotropic turbulence (HIT) is generated using the method of Rogallo [9]. This method defines the initial velocity field in a Fourier domain. The initial energy spectrum is chosen from the spectrum of Mansour & Wray [10]. The simulation of HIT is conducted in the domain of size $2\pi \times 2\pi \times 2\pi$ with the resolution of $128 \times 128 \times 128$.

The HIT simulation was performed until the energy spectrum follows the Kolmogorov spectrum with the slope of $\kappa^{-5/3}$ (where κ being the wavenumber) in the inertial subrange (Figure 2) before being combined with the vortex pair. Figure 3 illustrates the vortical structure of the HIT, visualised by the isosurface of the second invariant of the velocity gradient tensor,

$$Q = -\frac{1}{2} \frac{\partial u_i}{\partial x_j} \frac{\partial u_j}{\partial x_i} \quad (4)$$

At this time. The intensity of the ambient turbulence is characterised by the turbulent kinetic energy dissipation rate (ϵ), defined as

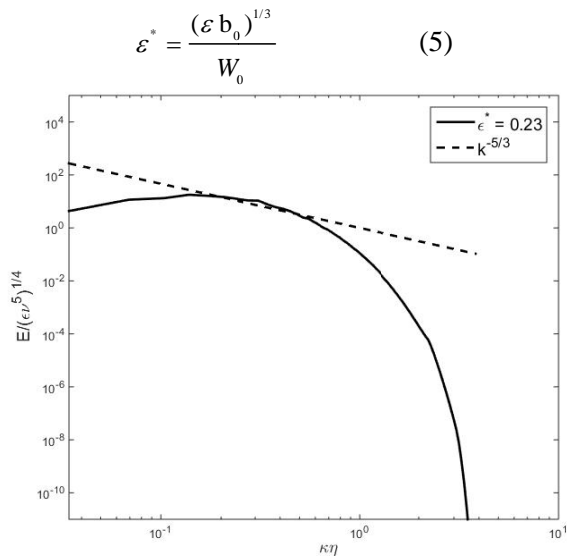


Figure2. Energy spectrum of HIT at the time before being combined with the vortex pair.

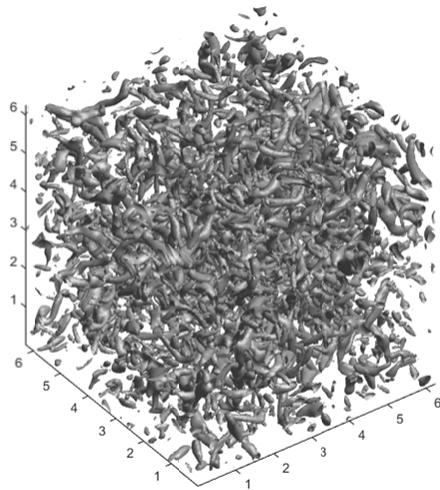


Figure3. Isosurface of the second invariant of the velocity graient tensor ($Q = 61.48$) illustrating the vortical structure of homogeneous isotropic turbulence at the time before being combined with the vortex pair.

The non-dimensional dissipation rate is chosen as $\varepsilon^* = 0.23$ corresponding to the moderate level of turbulence in a realistic ambient [11].

2.2. Combining the Vortex Pair and Ambient Turbulence

To combine the HIT and the vortex pair, the three identical turbulence fields are first stacked in the z -direction to adjust the domain size in that direction to 6π , as displayed in Figure 4. The vortex pair is then superimposed in the HIT using the superposition method of Rind [12]. The contour of the vorticity magnitude of the vortex

pair in the turbulence ambient is displayed in Figure 5.

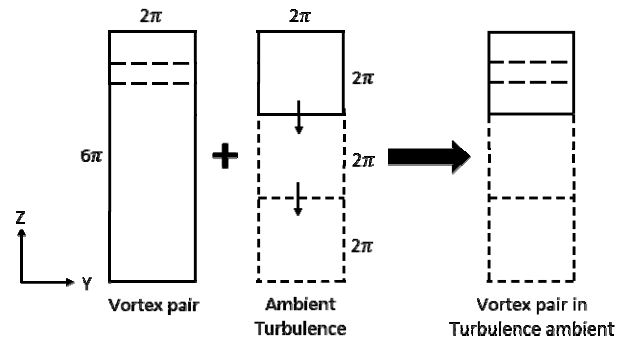


Figure4. Combination of the vortex pair domain and the turbulence domain.

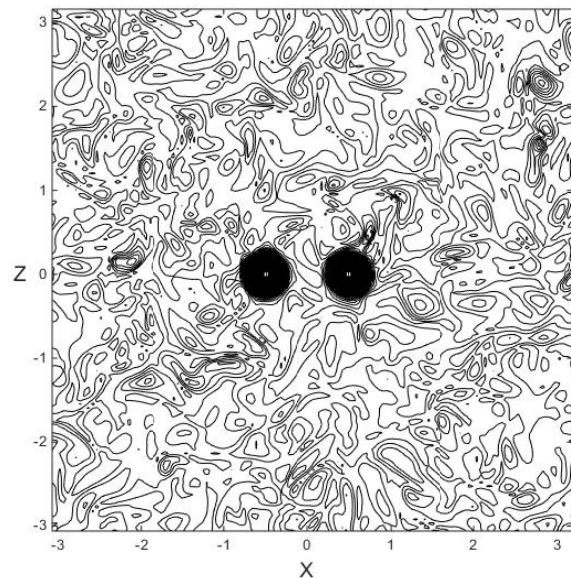


Figure 5. Contour of the vorticity magnitude of the vortex pair in the turbulence ambient at $t^* = 0.0$

3. Results

3.1. Flow Characteristic

Figure 6 and 7 respectively illustrate the flow characteristic of a vortex pair in a quiescent ($\varepsilon^* = 0.0$) and turbulence ambient ($\varepsilon^* = 0.23$), visualised by the isosurface of the second invariant of the velocity gradient tensor

As can be seen from Figure 6(a), the vortex pair in a quiescent background undergoes transition via the elliptical instability. It shows the sinusoidal manner with the wavenumber of about 6. As the flow develops further, the vortical structure looks more complex due to the development of the secondary vortex appearing in the transverse direction of the main flow, as shown in Figure 6(b). It causes the vortex pair to

weaken and then breakdown to turbulence. Eventually, the vortex pair rapidly decays and disappears, as shown in Figure 6(c).

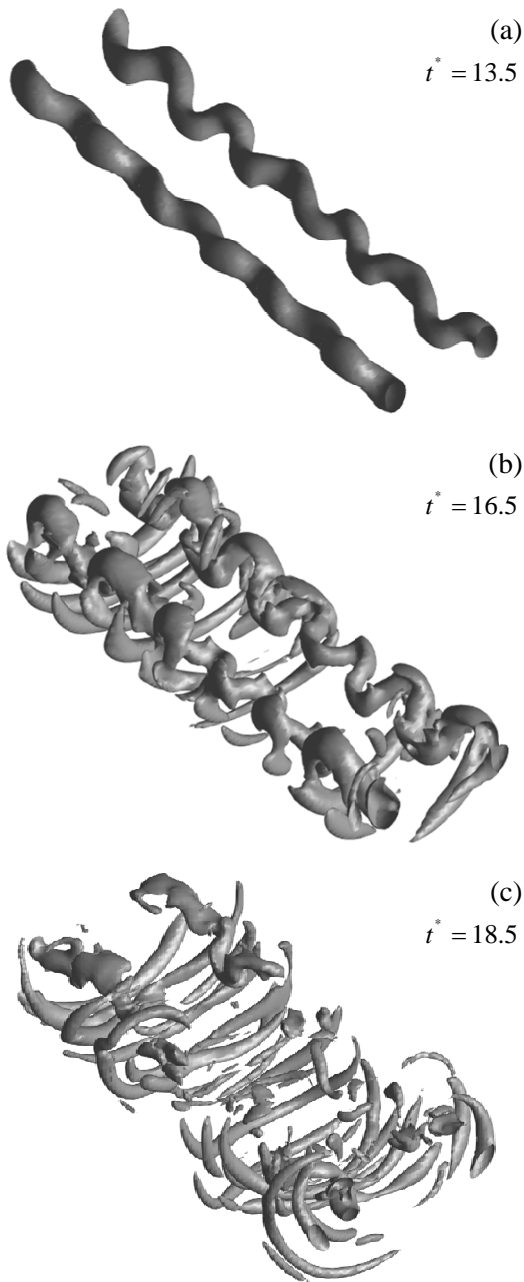


Figure 6. Isosurface of the second invariant of velocity gradient tensor ($Q = 87.49$) for $\varepsilon^* = 0.0$ at (a) $t^* = 13.5$, (b) $t^* = 16.5$ and (c) $t^* = 16.5$.

On the other hand, the moderate turbulence ambient accelerates the appearance of the secondary vortex (figure 7a). The characteristic of the elliptical instability cannot be observed suggesting that the linear instability might be bypassed. The size of the secondary vortex increases with time (figure 7b) causing the swift

breakdown and resulting in the rapid decay of the vortex strength. Finally, the vortex pair is destroyed (figure 7c).

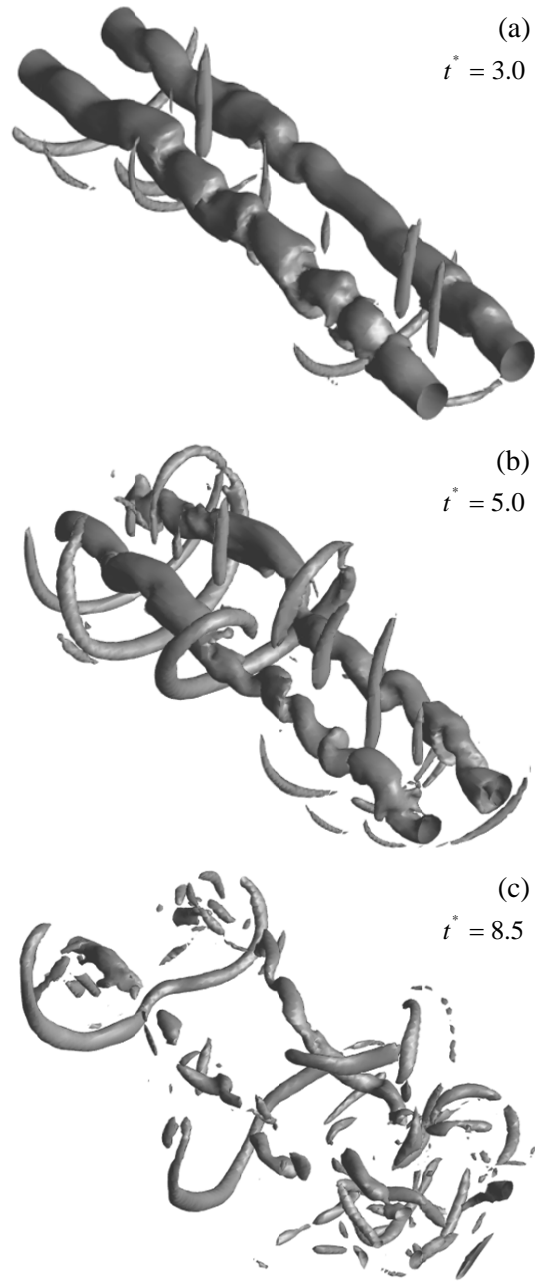


Figure 7. Isosurface of second invariant of velocity gradient tensor ($Q = 8.47$). For $\varepsilon^* = 0.23$ at (a) $t^* = 3.0$, (b) $t^* = 5.0$ and (c) $t^* = 8.5$

Figure 8 and 9 respectively show the time development of the vortex pair in a quiescent and turbulence ambient. It can be seen that the vortex pair in a quiescent ambient requires a longer time to breakdown to turbulence (figure 8f, $t^* \approx 15.0$) comparing to that in turbulence ambient (figure 9b, $t^* \approx 5.0$). When comparing both cases at the same time (figure 8b and figure 9b, at $t^* = 5.0$),

it can be seen that the vortex pairs for both cases are

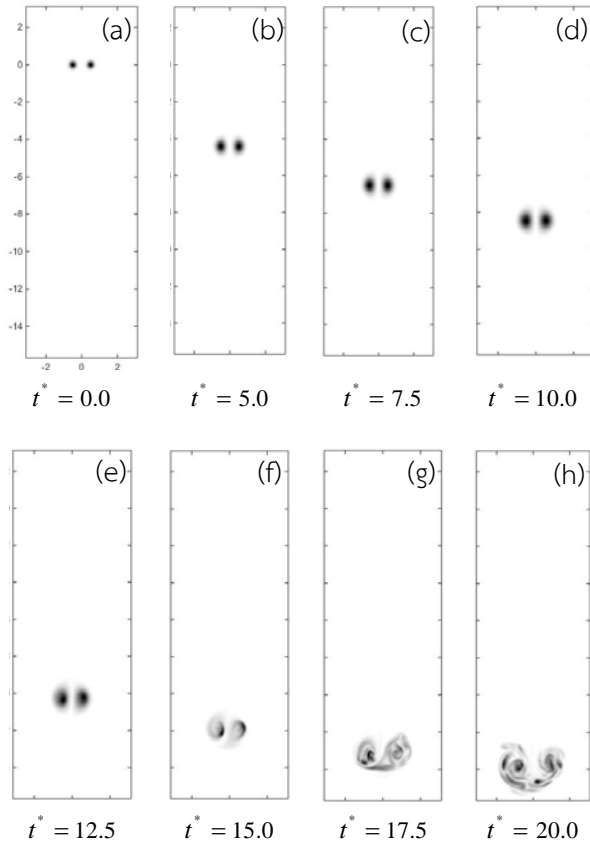


Figure8. Contour of vorticity magnitude of the vortex pair developing in the quiescent background ($\varepsilon^* = 0.0$) at $t^* = 0.0 - 20.0$.

in approximately the same descent height $z^* \approx -4.5$, but the three-dimensional instability does not seem to yet develop for the vortex pair in the quiescent ambient. Once the flow develops further, a vortex pair in a quiescent background drops to $z^* \approx -14.0$ at $t^* \approx 20.0$ (figure 8h), while the vortex core weakens and finally destroyed. In contrast, a vortex pair in a turbulence ambient is destroyed at higher distance $z^* \approx -6.5$ (figure 9e, $t^* \approx 12.5$) by the effect of viscosity and turbulence ambient.

3.2. Spectral Analysis

Figure 10 shows the evolution of the energy of the most amplified perturbation modes of a vortex pair in both quiescent ($\varepsilon^* = 0.0$) and turbulence ambients ($\varepsilon^* = 0.23$). For the vortex pair in a quiescent ambient, it develops both the linear and the nonlinear phases of the three-dimensional instability. The linear regime occurs between $t^* \approx 3.5$ (time when the energy starting to increase

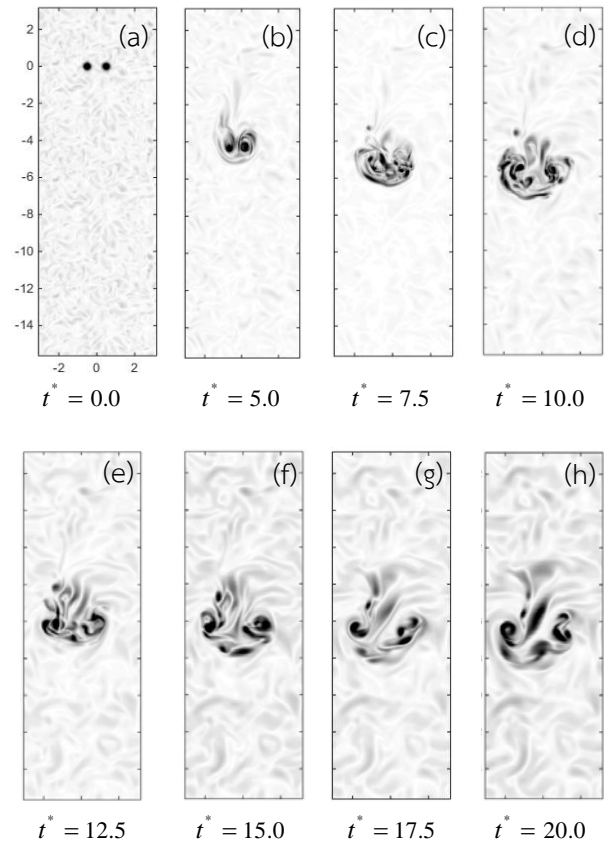


Figure9. Contour vorticity magnitude of a vortex pair developing in turbulence ambient ($\varepsilon^* = 0.23$) at $t^* = 0.0 - 20.0$ and $\omega = 0.6\omega_{\max}$.

from the minimum point) and $t^* \approx 12.5$ (time when the energy exceeding about 2% of the slope [5]). The most amplified mode is at the wavenumber of $\kappa = 6$ or at the wavelength of $\lambda = 1.04$, which corresponding to the breakdown due to the elliptical instability. This agrees very well with the work of Nomura et al. ($\kappa = 6.3, \lambda = 1.04$) [5] and Laporte & Corjon ($\lambda = 0.85 \pm 0.05$) [4]. The growth rate of the energy of each mode is computed from

$$\sigma_{\kappa} = \frac{1}{2} \left(\frac{d \ln E_{\kappa}}{dt} \right). \quad (7)$$

The growth rate of the most amplified mode ($\kappa = 6$) is 0.8432. This agrees well with the growth rate of Nomura et al. ($\sigma_{\kappa} = 0.83$) and Laporte & Corjon ($\sigma_{\kappa} = 0.96 \pm 0.3$). However, for the vortex pair in the ambient turbulence, the linear

instability phase cannot be observed. Therefore the

growth rate cannot be computed. The linear phase and the mode with the most energy changes to $\kappa = 2$ (not shown here), corresponding to the Crow's instability.

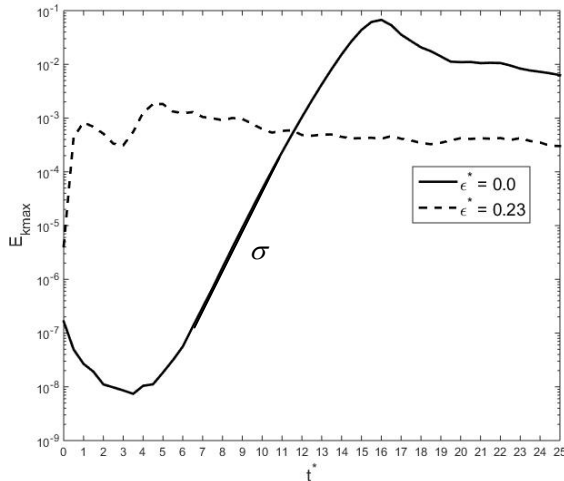


Figure 10. Development of the energy of the most amplified perturbation modes for the vortex pair in quiescent and turbulence backgrounds.

4. Conclusion

The effect of the ambient turbulence on the elliptical instability of a counter-rotating vortex pair is investigated by using direct numerical simulation. For the vortex pair in a quiescent background, it is found that the wavenumber of the most amplified mode is $\kappa = 6$ (wavelength of $\lambda = 1.04$) and the growth rate of this mode is $\sigma = 0.83$. This corresponds to the breakdown due to the elliptical instability. The vortex pair breaks down to turbulence at time $t^* \approx 15.0$. The turbulence ambient seems to accelerate the breakdown process. The vortex pair subject to the ambient turbulence begins to breakdown at time $t^* \approx 2.0$. The linear phase of the three-dimensional instabilities is bypassed and the most amplified mode is altered to mode $\kappa = 2$ (wavelength $\lambda = 3.14$).

5. Acknowledgments

The authors would like to thank the Faculty of Engineering, Chiang Mai University for the financial support and the use of computing facilities.

6. References

- [1] Meunier, P., Dizès, S.L. and Leweke, T. (2005). Physics of vortex merging, *C. R. Physique*, vol. 6, 2005, pp. 431–450.
- [2] Gerz, T., Holzappel, F. and Darracq, D. (2002). Commercial aircraft wake vortices, *Aerospace Sciences*, vol. 38, 2002, pp. 181–208.
- [3] Zurheide, F. and Schroder, W. (2007). Numerical Analysis of Wing Vortices, *Fluid Mechanics and Multidisciplinary Design*, vol. 96, 2007, pp. 17-25.
- [4] Laporte, F. and Corjon, A. (2000). Direct numerical simulations of the elliptic instability of a vortex pair, *Physics of Fluids*, vol. 12, 2000.
- [5] Nomura, K.K., Tsutsui, H., Mahoney, D. and Rottman, J.W. (2006). Short-wavelength instability and decay of a vortex pair in a stratified fluid, *J. Fluid Mech.*, vol. 553, 2009, pp. 283–322.
- [6] Misaka, T., Holzappel, F., Hennemann, I., Gerz, T. and Manhart, M. (2012). Vortex bursting and tracer transport of a counter-rotating vortex pair, *Phys. Fluids*, vol. 24, 2012.
- [7] Proctor, F.H., Ahmad, N.N., Switzer, G.S. and Duparcmeur, F.M.L. (2010). Three-Phased Wake Vortex Decay, *AIAA Atmospheric and Space Environments Conference*, Toronto, ON, AIAA-2010-7991, 2010.
- [8] Leweke, T., Dizes, S.L. and Williamson, C.H.K. (2016). Dynamics and instabilities of vortex pairs, *Annu. Rev. Fluid Mech*, vol. 48, 2016, pp. 1-35.
- [9] Rogallo, R.S. (1981). Numerical Experiment in Homogeneous Turbulence, *NASA Tech. Memo.*, 1981.
- [10] Mansour, N.N. and Wray, A.A. (1994). Decay of isotropic turbulence at low Reynolds number, *Physics of Fluids*, vol. 6, 1994.
- [11] Switzer, G.F. and Proctor, F.H. (2000). Numerical Study of Wake Vortex Behavior in Turbulent Domains with Ambient Stratification, *38th Aerospace Sciences Meeting and Exhibit*, Reno, NV, AIAA-2000-0755, 2000.
- [12] Rind, E. (2011), *Turbulent Wakes in Turbulent Streams*, PhD Thesis, University of Southampton.